PROOF UPGRADE FOR BI/MULTISTATIC RADAR OBSERVATION

Jens Rosebrock(1) and Michael Oswald(2)

(1) *FGAN-Research Institute for High Frequency Physics and Radar Techniques (FHR), Germany, Email: rosebrock@fgan.de*

(2) *Institute of Aerospace Systems, Technische Universität Braunschweig, Germany, Email: m.oswald@tu-bs.de*

ABSTRACT

An upgrade of the radar performance model used in ESA's Program for Radar and Optical Observation Forecasting (PROOF) is presented. The upgraded version computes detection probabilities for bi- and multistatic configurations and incoherent pulse integration. Both circular symmetric and arbitrary antenna patterns can be defined piecewise as one- or two-dimensional power sums. Furthermore, the change of attenuation due to the variation of the distances between the object and the transmitter and receiver, respectively, during the passage is taken into account. The motion vector of the passing object is assumed to be constant relative to each antenna during the passage, but arbitrary otherwise. An approach for analytical computation of the average total attenuation is given.

Key words: MASTER; PROOF; radar performance model; detection probability; incoherent pulse integration.

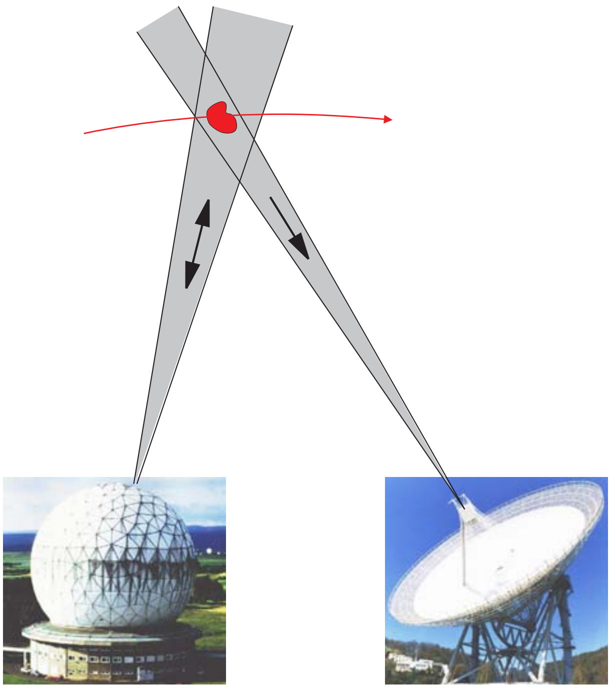

Figure 1. Passage of an object through two antenna beams.

1. INTRODUCTION

The steadily growing population of space debris is a risk for astronauts and operational space objects. For risk assessment models like ESA's Meteoroid and Space Debris Terrestrial Environment Reference Model (MASTER, (Bendisch et al., 2000a)) are required. These models have to be periodically updated in order to account for the dynamic changes of the population. There is a need to verify these updates by optical or radar observations obtained from repeated measurement campaigns. To this end averages and histograms derived from the observations are compared to corresponding values predicted from the model. In order to obtain these predictions, sensor performance models are required which derive the compared quantities from the debris model and the properties of the sensor. In particular, in the radar performance model detection probabilities are calculated for a specified passage of a debris object.

ESA's sensor performance model is called Program for Radar and Optical Observation Forecasting (PROOF, (Bendisch et al., 2000b)). PROOF contains performance models for optical and radar sensors. In the radar part of PROOF incoherent integration of N pulses is assumed. The case of coherent integration is simpler and can be treated like a single pulse. Detection probabilities are computed for each passage predicted by the MASTER model. Measured averages like radar cross section (RCS), height, Doppler inclination etc. are then computed from the data of passages provided by the MASTER model by weighting them with their detection probability.

In the past a monostatic radar sensor with a parabolic antenna was described in PROOF mainly by its beam width assuming an Airy pattern, which corresponds to a uniform field distribution on a circular aperture, and the noise equivalent RCS for a standard range (e.g. 1000 km). The RCS of the object was assumed as known and constant during the passage (Swerling case 0).

In a more general setup two arbitrary patterns of transmitting and receiving antennas are crossed by an object. Fig. 1 shows a bistatic setup with FGAN's TIRA and the Effelsberg radio telescope as an example. In Swerling case 0 which assumes a constant, known RCS and Swerling cases 1 and 3, where a random RCS is assumed constant during the passage, the detection probability de-

Proceedings of the Fourth European Conference on Space Debris, Darmstadt, Germany, 18-20 April 2005 (ESA SP-587, August 2005)

pends only on the averaged signal-to-noise ratio (SNR). The original single pulse signal-to-noise ratio, which is obtained if the direction of maximum gain points to the object for both antennas, has then to be multiplied by the energy or power attenuations of both antenna patterns and the attenuations caused by the varying ranges averaged over the part of the path corresponding to the integrated pulses to obtain an equivalent RCS for the case without attenuation. Fig. 2 shows an example for the varying total gain during a passage.

The analytical computation of the averaged attenuation and the computation of detection probabilities for these cases is described below for a constant velocity during the passage.

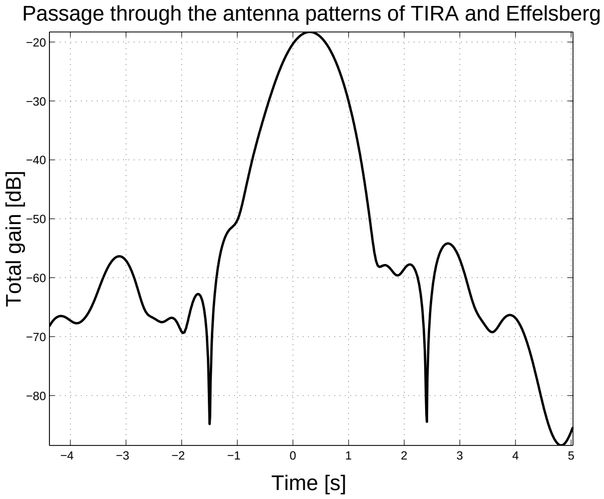

Figure 2. Example for the total gain during a passage relative to the maximum antenna gains (usually at the antenna axis) and the 1/range^2-factors at a given time (e.g. t=0).

2. DESCRIPTION OF ANTENNA PATTERNS

There are several possibilities to describe a general antenna pattern, e.g. by Jacobi-Bessel expansion. Two cases are pursued here:

1. Description of a general antenna pattern piecewise by two-dimensional polynomials.
2. Description of a circular symmetric antenna pattern piecewise by one-dimensional polynomials.

In the first case the arguments of the polynomials could be any quantities describing the direction of the line of sight (LOS, the line between the antenna and the object). It turns out that the coordinates x_P, y_P of the intersection P of the LOS with a plane orthogonal to the antenna axis leads to a simple solution of the SNR averaging problem. In the circular symmetric case the argument of the polynomials could be any parameter describing the angle between the LOS and the antenna axis. It turns out that $r_P^2 = x_P^2 + y_P^2$, the squared length of the distance between intersection point P and antenna axis leads to a tractable solution. Fig. 3 shows the definitions of these quantities.

For both cases the range varies with the arguments of the antenna pattern unlike antenna patterns given in the usual way, where the range remains constant. This has to be taken into account if a polynomial description is derived from a given antenna pattern.

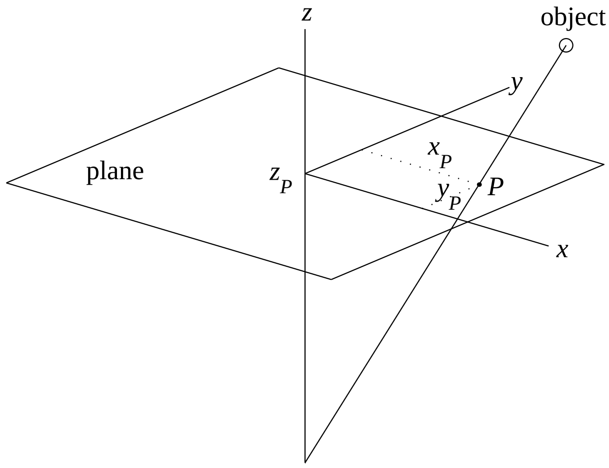

Figure 3. Arguments of the antenna pattern.

3. PASSAGE GEOMETRY AND ANTENNA GAIN

The velocity vector of a passing object is assumed to be constant during a passage. Then the range vector can be written as

$$\mathbf{z}(t) = \mathbf{z}_0 + \mathbf{z}_1 t, \tag{1}$$

where $\mathbf{z}_0$ is the position at $t = 0$ and $\mathbf{z}$ is the velocity vector. If a coordinate system is used, in which the z-direction coincides with the antenna axis and the origin coincides with the antenna location, in particular

$$\mathbf{z}(t) = \begin{pmatrix} x_0 \\ y_0 \\ z_0 \end{pmatrix} + \begin{pmatrix} \sin\alpha\cos\phi \\ \sin\alpha\sin\phi \\ \cos\alpha \end{pmatrix} vt, \tag{2}$$

where v is the velocity and α is the angle between the path and the antenna axis. The direction of the LOS is then defined by

$$\hat{x} := \frac{x}{z} = \frac{x_0 + x_1 t}{z_0 + z_1 t} \qquad \hat{y} := \frac{y}{z} = \frac{y_0 + y_1 t}{z_0 + z_1 t}. \tag{3}$$

Then a modified antenna gain function $f(\hat{x}, \hat{y})$ can be defined as

$$f(\hat{x}, \hat{y}) := \frac{z^2}{R^2} \cdot G(\hat{x}, \hat{y}), \tag{4}$$

where $R = \sqrt{x^2 + y^2 + z^2}$ is the range and $G(\hat{x}, \hat{y})$ is the usual antenna gain over isotropic radiator in the direction given by $\hat{x}$ and $\hat{y}$. This definition is justified by the fact that for a given direction the range R is proportional to z.

Inserting $\hat{x}$ and $\hat{y}$ from Eq. 3, temporal functions $G(t) := G(\hat{x}(t), \hat{y}(t))$ and $f(t) := f(\hat{x}(t), \hat{y}(t))$ are obtained.

4. SNR AVERAGING

4.1. SNR from antenna gains

Let $\sigma_{N,0}$ be the bistatic noise equivalent RCS for the range $R_0 := \sqrt{R_T \cdot R_R}$, where R_T is the range of the object with respect to the transmitter and R_R is the range of the object with respect to the receiver. By definition $\sigma_{N,0}$ is given for the case that for transmitter and receiver the direction of the antenna gain maximum is pointing to the object. For simplicity the transmitter power and the pulse length are assumed to be fixed. Then from Eq. 4 the SNR at time t becomes

$$\begin{aligned} SNR(t) &= \frac{G_T(t)G_R(t)}{G_{T,max}G_{R,max}} \frac{R_0^4}{R_T^2(t)R_R^2(t)} \frac{\sigma}{\sigma_{N,0}} \\ &= \frac{f_T(t)f_R(t)}{G_{T,max}G_{R,max}} \frac{R_0^4}{z_T^2(t)z_R^2(t)} \frac{\sigma}{\sigma_{N,0}} \end{aligned} \tag{5}$$

where σ is the true RCS. Defining a modified antenna gain relative to the maximum

$$g(\hat{x}, \hat{y}) := \frac{f(\hat{x}, \hat{y})}{G_{max}} = \frac{z^2}{R^2} \cdot \frac{G(\hat{x}, \hat{y})}{G_{max}}, \tag{6}$$

the SNR becomes

$$SNR(t) = R_0^4 \frac{\sigma}{\sigma_{N,0}} \frac{g_T(t)g_R(t)}{z_T^2(t)z_R^2(t)}. \tag{7}$$

Only the last factor varies with time and has to be averaged over time.

4.2. Time averaging for general antenna patterns

For general antenna patterns the function $g(\hat{x}, \hat{y})$ can be described piecewise as a polynomial in $\hat{x}$ and $\hat{y}$. Substituting Eq. 3 for the arguments, a rational expression results for $g(t)$. Since $z(t)$ is linear in t, also

$$\frac{g(t)}{z^2(t)} \tag{8}$$

and also the last factor of Eq. 7 are rational expressions in t. Integration over a time interval is accomplished by partial fraction expansion and integration of each term, which is possible analytically.

4.3. Time averaging for circular symmetric antenna patterns

For circular symmetric antenna patterns the symmetry is assumed around the axis z. The first idea would be to develop $g(\hat{x}, \hat{y})$ in powers of $\hat{r} := \sqrt{\hat{x}^2 + \hat{y}^2}$. But then, if $r(t)$ is inserted as the argument, $g(t)$ is no longer a rational expression in t. Therefore, it is much easier to develop $g(\hat{x}, \hat{y})$ in powers of $\hat{r}^2 = \hat{x}^2 + \hat{y}^2$ which is a polynomial in t:

$$\hat{r}^2 = C_r \cdot \frac{\hat{r}_0 + \hat{r}_1 t + t^2}{(\hat{z}_0 + t)^2} \tag{9}$$

with

$$\hat{r}_0 := \frac{x_0^2 + x_1^2}{x_1^2 + y_1^2}, \tag{10}$$

$$\hat{r}_1 := 2\frac{x_0 x_1 + y_0 y_1}{x_1^2 + y_1^2}, \tag{11}$$

and

$$C_r := \frac{x_1^2 + y_1^2}{z_1^2} = \tan^2 \alpha. \tag{12}$$

Therefore, also the expression 8 becomes rational.

4.4. Assignment of expansion regions to time intervals

4.4.1. General antenna patterns

In general, the boundaries between different expansion regions of the antenna patterns may have arbitrary shape. In this case the determination of time intervals depends on the description of the boundaries. In case that the expansion regions are convex polygons bounded by a set of straight lines, the intersections of the flight path (projected onto a plane orthogonal to the LOS) with each of the lines can be determined along with the corresponding intersection times. For each pair of subsequent intersection points the region corresponding to the line connecting them can be determined by taking an arbitrary point on the line and comparing it to half planes given by the other boundary lines. The search can be confined to the boundary lines of those regions, which have both intersected boundary lines in common.

A non-convex region can be described either by a union of convex regions or by the difference of its convex hull and a set of convex regions.

4.4.2. Circular symmetric antenna patterns

When an object passes an antenna pattern, the normalised distance $\hat{r}$ from the antenna axis first decreases to a minimum $\hat{r}_{min}$ and then increases. The time t_{min} of the minimum is obtained by setting the derivative of Eq. 9 to zero yielding

$$t_{min} = \frac{2\hat{r}_0 - \hat{z}_0\hat{r}_1}{2\hat{z}_0 - \hat{r}_1}. \tag{13}$$

Inserting this into Eq. 9 yields

$$\hat{r}_{min}^2 = \frac{(x_0 y_1 - x_1 y_0)^2}{|z_0 \mathbf{x}_1 - z_1 \mathbf{x}_0|^2}, \tag{14}$$

where $\mathbf{x}_i := (x_i, y_i)^\top$ for $i \in \{0, 1\}$.

Let $\{0, \hat{r}_1^2, \ldots, \hat{r}_N^2\}$ be the boundaries of the polynomial expansion intervals. For each $\hat{r}_1 \geq \hat{r}_{min}$ two solutions for the passage time t_i can be obtained as

$$t_{\pm i} = \frac{z_0 z_1 \hat{r}_i^2 - \mathbf{x}_0^T \mathbf{x}_1 \pm \sqrt{(\hat{r}_i^2 - \hat{r}_{min}^2)|z_0 \mathbf{x}_1 - z_1 \mathbf{x}_0|^2}}{|\mathbf{x}_1|^2 - z_1^2 \hat{r}_i^2} \tag{15}$$

by solving Eq. 9 for t. For each antenna, a set of time intervals is determined from the ordered set $\{t_{-N}, \ldots, t_{-n}, t_{min}, t_n, \ldots, t_N\}$ of boundary times where n is defined by $\hat{r}_n > \hat{r}_{min}$ and $\hat{r}_{n-1} \leq \hat{r}_{min}$. The intersection of the time intervals of transmitter and receiver yields a set of time intervals which have to be treated separately for total gain integration.

4.5. Paths nearly orthogonal to the LOS

In the usual case, when the range is nearly constant during the passage ($z_1 \cdot T_{Passage} \ll z_0$), numerical problems arise with partial fraction expansion since then total gain as a function of times has to be described by a linear combination of terms which are almost constant during the passage. Therefore, small differences of large terms are likely to be used. As a remedy for these problems the reciprocal of each arising term

$$\frac{1}{(\hat{z}_0 + t)^n}$$

in the expression for $\hat{r}^{2n}$ is expanded in a power series. The required number of summands for a certain relative precision is

$$\frac{nT_{rel} - 1}{1 - T_{rel}} + \text{const}$$

where

$$T_{rel} = \frac{2 z_1 T_{Passage}}{z_0}. \tag{16}$$

The coefficients can be determined by recursion for each n separately.

5. DETECTION PROBABILITIES

5.1. Incoherent integration

It is quite unlikely that an object changes its RCS during a passage. Only for rapid tumbling objects this would be the case. Therefore, only Swerling cases 0, 1, and 3 are considered. For these cases under a square law detector assumption, the detection probability for a given number N of incoherently integrated pulses depends only on E_{sum}, the total SNR, i.e. the ratio of the integrated signal energy (or the expectation thereof) to the noise energy of both quadrature components of a single pulse:

$$E_{sum} = \sum_{n=1}^{N} SNR(n) = N \cdot \overline{SNR} \tag{17}$$

In Swerling cases 1 and 3 the signal energy is replaced by its expectation $\overline{E_{sum}}$. Shnidman (Shnidman, 1995) gives a concise derivation of detection probabilities. General expressions are given there in Eq. 22 and 23 for Swerling case 0 and in Eq. 25 for all other Swerling cases and more explicit in Eq. 81 – 85. Alternative expressions can be found in Appendix A of (Meyer & Mayer, 1973). Some manipulations on these expressions (Rosebrock et al., 1999) lead to

$$\begin{aligned} P_d &= \sum_{k=0}^{\infty} e^{-E_{sum}} E_{sum}^k \frac{1}{k!} \sum_{l=0}^{N-1+k} e^{-T} \frac{T^l}{l!} && (18) \\ &= 1 - \sum_{l=0}^{\infty} e^{-T} \frac{T^l}{l!} \sum_{k=0}^{l-N} e^{-E_{sum}} E_{sum}^k \frac{1}{k!} && (19) \end{aligned}$$

for Swerling case 0, where T is the detection threshold for the sum of detector outputs. The first equation is preferred if $E_{sum} < T$ and the second otherwise. The false alarm probability P_{fa} is obtained by inserting $E_{sum} = 0$. Then the summation over k reduces to a single term for $k = 0$. For Swerling case 1

$$P_d = e^{-T} \left[\sum_{k=0}^{N-1} \frac{T^k}{k!} + \sum_{k=N}^{\infty} \frac{T^k}{k!} \left(\frac{E'}{E'+1} \right)^{k-N+1} \right] \tag{20}$$

is the preferred expression for $E' := \overline{E_{sum}} < T$, where the first term corresponds to P_{fa}, and

$$P_d = 1 - e^{-T} \sum_{k=N}^{\infty} \frac{T^k}{k!} \left[1 - \left(\frac{E'}{E'+1} \right)^{k-N+1} \right] \tag{21}$$

for $E' > T$. For Swerling case 3

$$\begin{aligned} P_d &= e^{-T} \left[\sum_{k=0}^{N-1} \frac{T^k}{k!} + \frac{c_1(1-c_1)T^N}{(N-1)!} \right. \\ &\quad \left. + c_2 \sum_{k=N}^{\infty} \frac{T^k}{k!} (1-c_1)^{k-N+1} \right] && (22) \end{aligned}$$

is preferred for $E' := \overline{E_{sum}}/2 < T$ where the first term again corresponds to P_{fa} and

$$\begin{aligned} P_d &= e^{-T} \left[\frac{c_1 T^{N-1}}{(N-2)!} + \sum_{k=0}^{N-2} \frac{T^k}{k!} \left(1 - c_3(1-c_1)^k \right) \right] \\ &\quad + c_3 e^{-c_1 T} && (23) \end{aligned}$$

for $E' > T$ with the following abbreviations:

$$c_1 := \frac{1}{1+E'}$$

$$
\begin{aligned}
c_2 &:= (1-(N-1)c_1 + c_1(1-c_1)T) \\
c_3 &:= \frac{c_2}{(1-c_1)^{N-1}}.
\end{aligned} \tag{24}
$$

5.2. Coherent integration

For coherent integration of pulses the range variations must be known so exact that uncertainty about the phase differences from pulse to pulse can be neglected. This means that range rate and further derivatives of the range as a function of time have to be determined with sufficient precision. If these conditions are met, the coherent integration can be conceived as a single matched filter operation. Correspondingly all Swerling cases treated above can be applied for $N = 1$ if the ratio of total signal energy (or the expectation thereof) and total noise energy is substituted for the SNR. The simplified expressions

$$P_d = e^{-\frac{T}{1+E'}} \tag{25}$$

with $E' = \overline{SNR}$ for Swerling case 1 and

$$P_d = \left(1 - \frac{E'T}{(1+E')^2}\right) e^{-\frac{T}{1+E'}} \tag{26}$$

with $E' = \overline{SNR}/2$ for Swerling case 3 arise. In contrast to incoherent integration, here the amplitude rather than energy gain has to be averaged. Analytical averaging is possible by methods similar to those employed for incoherent integration.

5.3. Multistatic setup

In multistatic constellations, for all bistatic transmitter–receiver pairs detection probabilities can be computed as outlined above. If all the detections are taken in common, the largest of these detection probabilities is a lower bound to the total detection probability at a false alarm rate at most multiplied by the number of receivers.

6. SENSOR PARAMETERS

In the past the sensor was described by the antenna beam width, transmitter power, pulse length, pulse period, wavelength, and the single pulse noise equivalent RCS at given range, transmitter power, and pulse length. In the presented model the noise equivalent RCS has to be given for each bistatic pair of transmitter and receiver. The antenna patterns are no longer described by their width, but by the boundaries of expansion regions and the expansion coefficients.

7. CONCLUSION

Methods for computing the detection probability of a passage have been derived under the assumption of constant RCS during the passage. Rather general patterns for both transmitter and receiver antennas can be used. The range variation during the passage is accounted for and integrated into the computation. A closed-form solution is possible for the required averaging of the SNR, but not always numerically stable. The modified radar performance model of PROOF will enable the validation of the MASTER model in more general situations than those which were possible in the past.

ACKNOWLEDGMENTS

The software PROOF was developed under ESA contract 18014/03/D/HK(SC). Responsibility for the contents resides in the authors who prepared this paper.

REFERENCES

Bendisch, J., Krag, H., Rex, D., Brandt, T., Sdunnus, H., Rosebrock, J., and Schildknecht, T., May 2000a, *Extension of ESA's MASTER Model to predict debris detections*. Final Report of Study Contract 12569/97/D/IM, ESA/ESOC, Darmstadt, Germany, 165 p. + CD-ROM.

Bendisch, J., Krag, H., Rex, D., Wegemann, R., Wegener, P., Wiedemann, C., Brandt, T., Bunte, K., Hauptmann, S., Sdunnus, H., and Walker, R., May 2000b, *Upgrade of ESA's MASTER Model*. Final Report of Study Contract 12318/97/D/IM, ESA/ESOC, Darmstadt, Germany, 267 p.+ CD-ROM.

Meyer, D. P. and Mayer, H. A., 1973, *Radar Target Detection. Handbook of Theory and Practice*. Academic Press, ISBN 0-12-492850-1 edition.

Rosebrock, J., Leushacke, L., and Mehrholz, D., October 1999, *Cooperative debris tracking and development of algorithms for mid-size debris detection with radar*. Final Report of Study Contracts 12248/97/D/IM and 12247/97/D/IM, ESA/ESOC, Darmstadt, Germany.

Shnidman, D. A., July 1995, Radar Detection Probabilities and Their Calculation. *IEEE Transactions on Aerospace and Electronic Systems*, 31(3):928 – 950.